

Kalman filtering and time-frequency distribution of random signals

P.G. Madhavan and W.J. Williams

Electrical Engineering & Computer Science Department
University of Michigan, Ann Arbor
1310 Beal Avenue, Ann Arbor, MI 48109
email: pgmadhav@eecs.umich.edu

ABSTRACT

A new method to estimate the energy distribution over the time-frequency plane of time-varying stochastic signals is presented. A state space modeling approach is used to represent the signal. A Kalman-smoothing algorithm is used to estimate the states from which the so-called "Kalman-smoothed time frequency distribution (KS-TFD)" is obtained. The KS-TFD estimate is positive, has good cross-term properties and high temporal resolution. The Kalman smoother-based estimates are optimal in the mean square sense and therefore the KS-TFD estimate has excellent noise performance. We demonstrate the "localizing" property of KS-TFD using deterministic signals such as impulses and Gabor logons. Minimum interference is seen with multi component signals. For Gabor logons buried in white noise at various signal-to-noise ratios, we show the excellent performance of the KS-TFD estimate in comparison to the non-causal spectrogram using quantitative performance indices.

Keywords: time-frequency distribution, Kalman filtering, random signals, state-space model.

2. INTRODUCTION

The methods of time frequency distributions (TFDs) for nonstationary signal analysis have seen significant amount of theoretical development in recent years^{1,2,3}. The methods of TFD have shown considerable promise in many application areas also⁴. However, it is fair to say that the development of a comprehensive and coherent theory of time frequency analysis for random signals and its application to the analysis of random signals or deterministic signals in the presence of random noise has not been forthcoming⁵.

In this article, we propose a linear, time-varying, stochastic state-space model for a discrete-time signal. The state-space model is chosen in such a fashion that the estimation of the TFD from the time-varying states of the model is straight-forward. The states of the model can be efficiently estimated by the Kalman filtering and Kalman smoothing algorithms. The states so estimated are the time-varying discrete Fourier transform coefficients. The magnitude-squared time-varying states are called "the Kalman-smoothed time frequency distribution (KS-TFD)".

We test the properties of the KS-TFD with a variety of deterministic signals as well as signals in the presence of white noise. Comparisons are made to Wigner distribution and the non-causal spectrogram which demonstrate the ability of KS-TFD to perform in low signal-to-noise ratio situations.

3. METHOD

Consider a general state space model of a time-varying stochastic signal, $y(n)$, as given below.

$$\underline{X}(n+1) = \underline{A}_n \underline{X}(n) + \underline{w}(n) \quad (1)$$

$$y(n) = \underline{\Phi}_n^T \underline{X}(n) + e(n) \quad (2)$$

For arbitrary choice of the matrix, \underline{A}_n , and the vector, $\underline{\Phi}_n$, equations (1) and (2) are together sometimes referred to as a time-variable parameter (TVP) model of a stochastic time series⁶. We define $\underline{X}(n)$ as follows and make the following special choice for the vector, $\underline{\Phi}_n$.

$$\underline{X}(n) = [X_1(n) \dots X_k(n) \dots X_M(n)]^T ; \quad \underline{\Phi}_n = \frac{1}{M} \begin{bmatrix} 1 & \dots & e^{j\frac{2\pi}{M}nk} & \dots & e^{j\frac{2\pi}{M}n(M-1)} \end{bmatrix}^T \quad (3)$$

In the noise-free observation case, $y(n)$ can be written as follows.

$$y(n) = \underline{\Phi}_n^T \underline{X}(n) = \frac{1}{M} \sum_{k=0}^{M-1} e^{j\frac{2\pi}{M}nk} X_k(n) \quad (4)$$

Equation (4) can be seen to be the (inverse of the) Goertzel algorithm⁷ where $X_k(n)|_{n=M}$ is the kth coefficient of the M-point DFT of the finite-duration sequence, $y(n)$, $0 \leq n \leq (M-1)$ or $\underline{X}(n)$ is the vector of all M-point DFT coefficients of $\{y(n-M+1), \dots, y(n)\}$.

An alternate way to consider equation (4) is by comparison with the Cramer spectral representation when $y(n)$ is restricted to being wide-sense stationary^{8,9}. The Cramer representation of $y(n)$ can be written as follows.

$$y(n) = \frac{1}{2\pi} \int_{-\pi}^{\pi} e^{j\omega n} dZ(\omega) \quad (5)$$

The increment process $\{dZ(\omega)\}$ has the properties that its energy at different frequencies is uncorrelated and that the expected value of $|dZ(\omega)|^2$ defines the spectrum, $S_y(\omega)d\omega$. Analogous to $|dZ(\omega)|^2$, for the nonstationary case in equation (4), we can define a time-varying spectrum based on $\underline{X}(n)$. We proceed as follows.

Assume that in equations (1) and (2), $e(n)$ and $w(n)$ are zero-mean Gaussian white noise sequences such that $E[e(i) w(j)] = 0$ for all i and j and the initial "state", $\underline{X}(0)$ is independent of $e(i)$ and $w(j)$. In the case where N samples of $y(n)$ are available, $\underline{X}(n)$, can be estimated by Kalman filtering and smoothing algorithms to obtain $\underline{X}(n|N)$ ^{6,10,11}. Specifically, given a noisy observation, $y(n)$, the Kalman smoother allows us to obtain the estimates, $\underline{X}(n|N)$, which are the estimated DFT coefficients for the sample instant, n . The variations of the DFT coefficients over time can be used to estimate the time-frequency distribution^{1,2}. Considering the individual elements of the state vector, we define the Kalman-smoothed time-frequency distribution (KS-TFD) as follows.

$$S_{KS}(k,n) = |X_k(n|N)|^2 \quad \text{for } n=1,2,\dots,N; \quad k=1,2,\dots,M \quad (6)$$

It can be shown that for the special choices of $A_n = I$, the identity matrix and $e(n) = 0$ in equations (1) and (2) and the state estimation algorithm as the *Kalman filter algorithm* instead of the *smoothing algorithm*, the estimate in equation (6) reduces to the well-known spectrogram. Therefore, the advantages of the KS-TFD estimate, $S_{KS}(k,n)$ over and above the spectrogram stem from the use of the Kalman smoothing algorithm which allows for increased temporal localization, the inclusion of $e(n)$ in equation (2) which permits the estimation of TFD of signals in the presence of noise and the appropriate choice of A_n to model the rapid variations in the spectral content. In the next section, we demonstrate the first two properties. Possible choices of A_n and their effects on the TFD estimate will be addressed in a later article.

4. SIMULATIONS

In the following tests, the evolution of the "state" vector, $\underline{X}(n)$, in equation (1) has been modeled by a random-walk model with the choice of A_n as the identity matrix. The so-called "time-variable parameter" (TVP) algorithm of Young⁶ was used to obtain the estimates of the states. The prediction, correction and fixed-interval smoothing¹⁰ algorithms are given below. The variables in the algorithm are as follows: $y(n)$ - observation scalar; A_n - state transition matrix; $Q(n)$ - process noise correlation matrix; σ_e^2 - measurement noise variance; $Q_r(n) = Q(n)/\sigma_e^2$; $\hat{X}(n|n-1)$ - estimate of predicted state at n ; $\hat{X}(n)$ - estimate of filtered state at n ; $\alpha(n)$ - innovations scalar; ϕ_n - measurement vector; $P(n|n-1)$ - correlation matrix of state prediction error.

Prediction:

$$\begin{aligned}\hat{X}(n|n-1) &= \underline{A}_n \hat{X}(n-1) \\ P(n|n-1) &= \underline{A}_n P(n-1) \underline{A}_n^T + \underline{Q}_e(n)\end{aligned}$$

Correction:

$$\begin{aligned}\alpha(n) &= y(n) - \underline{\phi}_n^T \hat{X}(n|n-1) \\ \beta(n) &= 1 + \underline{\phi}_n^T P(n|n-1) \underline{\phi}_n \\ \hat{X}(n) &= \hat{X}(n|n-1) + P(n|n-1) \underline{\phi}_n \frac{\alpha(n)}{\beta(n)} \\ P(n) &= P(n|n-1) - P(n|n-1) \underline{\phi}_n \underline{\phi}_n^T P(n|n-1) \frac{1}{\beta(n)}\end{aligned}$$

Smoothing:

$$\begin{aligned}L(n-1) &= \left[I - P(n) \underline{\phi}_n \underline{\phi}_n^T \right] \left[\underline{A}_n^T L(n) - \underline{\phi}_n \left(y(n) - \underline{\phi}_n^T \underline{A}_{n-1} \hat{X}(n-1) \right) \right] \\ \hat{X}(n|N) &= \underline{A}_n^{-1} \left[\hat{X}(n+1|N) + \underline{Q}_e(n) L(n-1) \right]\end{aligned}$$

Initialization:

$$\hat{X}(0) = \underline{0}; \quad P(0) = cI; \quad L(N) = \underline{0}; \quad \underline{Q}_e(n) = \frac{Q(n)}{\sigma_e^2} = rI$$

Here, c, r = small positive constants and N is the total number of data points.

The following simulations were conducted -

Test(1): impulse signal, i.e., $y(n)=\delta(n-50)$;

Test (2): sum of 2 Gabor logons, $s(n)=s_1(n)+s_2(n)$ where for $k=1,2$ and logon location parameters, (n_k, ω_k) , $s_k(n)$ is defined as follows.

$$s_k(n) = \frac{\pi^{3/4}}{\sqrt{\sigma}} e^{-\frac{1}{\sigma^2}(n-n_k)^2} e^{j\omega_k n}$$

Test (3): $x(n)$, signal in additive white Gaussian noise, i.e., sum a Gabor logon, $s_j(n)$ at a new location, (n_j, ω_j) and white noise, $w(n)$, with various signal-to-noise ratios.

Qualitative Analysis:

The results are shown in figures 1 to 3. All the figures show the time series on the top row and the mesh plot of $S_{KS}(k,n)$ immediately below. In figure 3, the bottom row shows the non-causal spectrogram of $x(n)$ for a rectangular window centered at n . The frequency axis spans the 0 to π range of the normalized discrete frequency. In figure 3, the location of the single Gabor logon is in the center of the time-frequency plane. Some qualitative features of these plots are discussed first.

The "localization" property of the KS-TFD estimate is demonstrated in figure 1. The KS-TFD estimate produces a clear broad-band peak at $n=50$. In comparison, the spectrogram that uses a rectangular window centered at n will have a step that extends from $n=50-(M/2)$ to $50+(M/2)$ where M is the window length with no clear peak (choices of window other than rectangular can be found in specific situations that have better localization property).

In figure 2, the KS-TFD estimate displays some of the desirable properties of a TFD estimate such as positivity and minimum cross-terms. We will compare the KS-TFD estimate to the Wigner distribution of $s_k(n)$, $W_k(n,\omega)$.

$$W_k(n,\omega) = e^{-\frac{1}{\sigma^2}(n-n_k)^2} e^{-\sigma^2(\omega-\omega_k)^2}$$

Consider the "ideal" TFD estimate as the *linear superposition* of the two Wigner distributions, i.e., $W(n,\omega) = W_1(n,\omega) + W_2(n,\omega)$, thereby eliminating the cross-terms. Obviously, $W(n,\omega)$ is an "ideal" estimate only in the case of logons well-separated in the time-frequency domain. The mean-squared error between $W(n,\omega)$ and the KS-TFD estimate normalized by the variance of $W(n,\omega)$ was found to be equal to 0.0019. Such a low normalized mean-squared error ($\approx 0.2\%$) implies that the KS-TFD estimate has the properties of minimum time-bandwidth product and positivity of Wigner distribution for one Gabor logon and lack of cross-terms of $W(n,\omega)$ as defined above.

The qualitative effect of added white noise at 0db SNR can be seen in the plots in figure 3. The "ideal" TFD estimate of $x(n)$ will be the Wigner distribution of a single Gabor logon similar to the ones in figure 2, but in this case located at the center of the time-frequency plane. The $S_{KS}(k,n)$ estimate in middle row is remarkably similar to this ideal result, showing qualitatively that our Kalman filter formulation allows for optimal estimation in the presence of additive noise. As a comparison to a traditional method, we chose the non-causal spectrogram since it also results in non-negative distributions, as shown in the bottom row. Clearly, the $S_{KS}(k,n)$ estimate is much

superior to the spectrogram.

A clearer picture of the comparisons among the Wigner distribution, KS-TFD estimate and non-causal spectrogram of the single Gabor logon can be obtained in we consider the "maximal energy" slice (which in this case is the 5th frequency slice) of the TFD of a single realization. In figure 4, the visual comparison among these 3 plots show two desirable properties of the KS-TFD estimate over the spectrogram. The first feature that can be noted is that the KS-TFD estimate (dashed line) is "closer" to the theoretical (solid line) than the spectrogram estimate (dash-dot line). (It should be pointed out that the "narrower" appearance of the spectrogram for this realization is not a consistent observation across the ensemble). In addition, the KS-TFD estimate is seen to be "smoother" than the spectrogram estimate with fewer "false" peaks. In the following section, we develop a performance index that captures both these properties and compare the KS-TFD and the spectrogram estimates for various signal-to-noise ratios.

Quantitative Analysis:

It is customary to utilize smoothness functionals in developing desirable performance criteria to be minimized so as to find an approximating function, F [], relating noisy data, x_i to desired data, d_i . A typical smoothness functional¹² is of the following form where the first term is the mean squared error and the second term is a smoothness functional which utilizes an nth-order differential operator.

$$H[F] = \frac{1}{N} \sum_{i=1}^N (F[x_i] - d_i)^2 + \int \left| \frac{d^n}{dx^n} F[x_i] \right|^2 dx$$

Similar to the smoothness functional above, we use a performance index which is the sum of mean-squared error and smoothness measure based on 1st and 2nd derivatives, averaged over the entire time-frequency plane.

$$I = MSE[W(k,n); S_{KS}(k,n)] + \sum_{k=1}^M MS[Sd1(k)] + MS[Sd2(k)]$$

Here, $Sd1(k) = S_{KS}(k,n) - S_{KS}(k,n-1)$ and $Sd2(k) = Sd1(k,n) - Sd1(k,n-1)$; the operators, $MSE[]$ calculates the mean-squared error between the arguments and $MS[]$ calculates the mean-squared value; M is the total number of frequency samples. The **normalized performance index**, NI , is obtained by normalizing the terms of performance index, I , by the variance and mean-squared value of the 1st and 2nd differences of $W(k,n)$. From the definition, it can be seen that smaller values of NI for a certain estimate indicate better performance in the sense that the estimate is "closer" to the theoretical TFD and that the estimate is "smoother".

The normalized performance index, NI, was calculated for 30 independent noise realizations at +3db, 0db and -3db SNRs. The average values of NI and the ratios of average NI of non-causal spectrogram to KS-TFD for the different SNRs are given in Table 1.

Table 1. Ensemble Performance Comparison of KS-TFD and non-causal spectrogram (*NCS)

SNR	Estimation Method	Average NI	Ratio
+3db	KS-TFD	1.309	6.3
	*NCS	8.2501	
0db	KS-TFD	1.8162	7.15
	NCS	12.9841	
-3db	KS-TFD	3.8266	8.97
	NCS	34.3225	

5. DISCUSSION

The ratio of average normalized performance index given in the last column of Table 1 is plotted in figure 5. The ratios can be interpreted to mean, for example at a 0db signal-to-noise ratio, the KS-TFD is over 7 times better (in the sense of being closer to the true TFD and smoother) than the non-causal spectrogram. In figure 5, it can also be seen that the superiority in performance of KS-TFD *increases as signal-to-noise ratio decreases*. This is consistent with our expectations since the spectrogram has no special ability to handle noise whereas the Kalman filter algorithm is optimal in the estimation of states in the presence of observation noise.

Based on the qualitative and quantitative analyses above, some general conclusions can be drawn about the properties of the KS-TFD estimate of time frequency distribution of signals in the presence of noise. The KS-TFD estimate is positive, has good cross-term properties and has high temporal resolution. A central feature of our method is the special choice of the "observation vector", ϕ_n , which is pre-determined. The pre-determination of vector, ϕ_n , assures that the Kalman smoother-based estimates are optimal. Therefore, the KS-TFD estimate will have the best possible noise performance.

It should be pointed out that one may observe equivalent results using other approaches, but the KS-TFD viewpoint provides a unifying framework. An example of this was pointed out in section 3 where the spectrogram approach can be seen as a special case of the KS-TFD method.

It should be noted that many alternate Kalman smoothing algorithms are available, some of which may have better performance than the one we have presented here.

The Kalman-smoothed time frequency distribution provides an effective method to model the energy distribution over the time-frequency plane of time-varying stochastic signals using the state space formulation. The additive combination of signal and white noise is only a basic application of this method - different formulations of the state evolution and observation noise will extend the applicability to cases such as signal in colored noise as well as non-stationary stochastic signals.

6. ACKNOWLEDGEMENT

We are grateful to Professor P. Khargonekar for the many useful discussions on Kalman filtering and to Professor A. Hero III for discussions on Cramer spectral representation.

7. REFERENCES

1. Cohen, L., "Time-frequency distributions - a review", *Proc. IEEE*, vol. 77, pp 941-981, 1989.
2. Williams, W.J. and Jeong, J., "New time-frequency distributions for the analysis of multicomponent signals", *Proc. SPIE*, vol. 1152, pp 483-495, 1989.
3. Hlawatsch, F. and Boudreault-Bartels, G.F., "Linear and quadratic time-frequency signal representations", *IEEE Signal Processing Magazine*, vol. 9, pp 21-67, 1992.
4. Cohen, L., *Time Frequency Analysis*, Prentice-Hall, New Jersey, 1995.
5. Porat, B., *Digital Processing of Random Signals*, Prentice-Hall, New Jersey, 1994.
6. Young, P., "Time variable and state dependent modelling of non-stationary and nonlinear time series", in *Developments in Time Series Analysis*, Subba Rao, T. (ed), Chapman & Hall, London, 1993.
7. Oppenheim, A.V. and Schafer, R.W., *Discrete-Time Signal Processing*, Prentice Hall, New Jersey, 1989.
8. Haykin, S., *Adaptive Filter Theory*, 3rd edition, Prentice-Hall, New Jersey, 1996.
9. Thomson, D.J., "Spectral estimation and harmonic analysis", *Proc. IEEE*, vol. 70, pp 1055-1096, 1982.
10. Gelb, A., Kasper, J.F., Nash, R.A., Price, C.F. and Sutherland, A.A., *Applied Optimal Estimation*, MIT Press, Massachusetts, 1974.
11. Kalman, R.E., "A new approach to linear filtering and prediction problems", *ASME Trans., J. Basic Eng.*, vol. 83-D, pp 95-108, 1960.
12. Poggio, T. And Girosi, F., "Networks for approximation and learning", *Proc. IEEE*, vol. 78, pp 1481-1497, 1990.

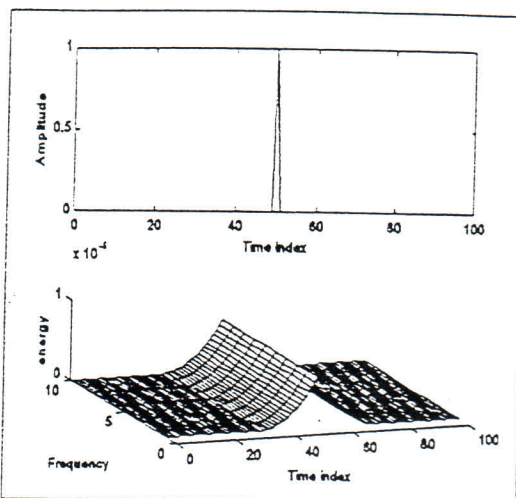


Figure 1. KS-TFD of an impulse

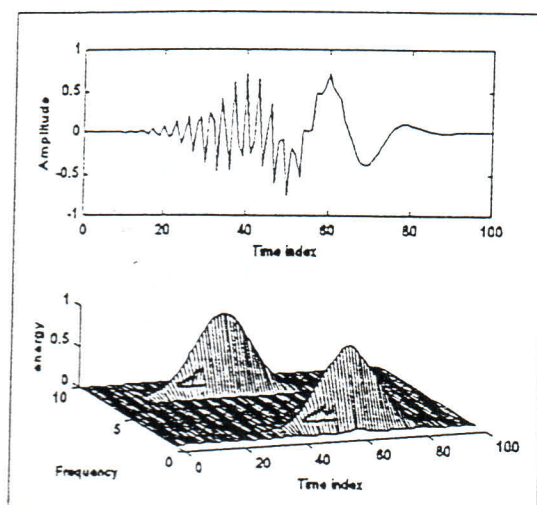


Figure 2. KS-TFD of 2 Gabor-logons

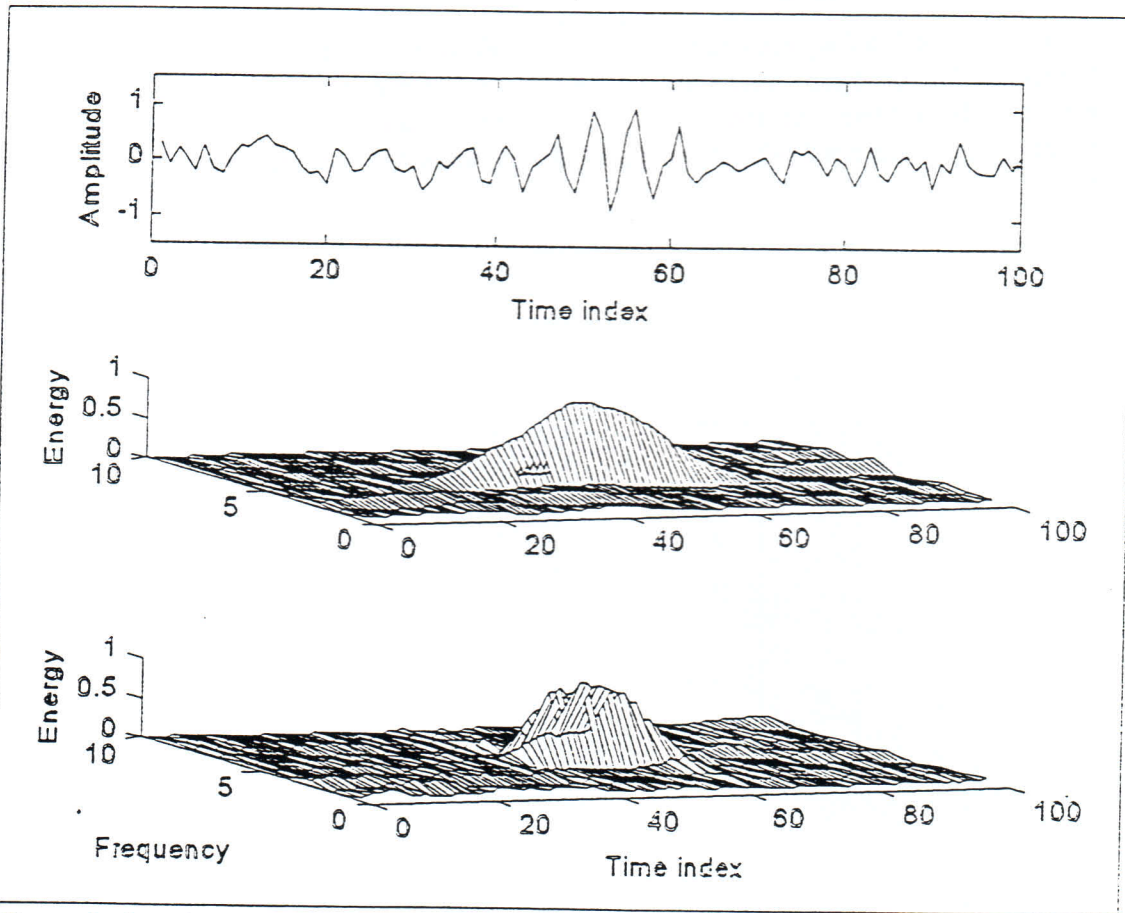


Figure 3. One Gabor logon, located at the center of the time-frequency plane, in white noise at 0db SNR; KS-TFD (middle row) and non-causal spectrogram (bottom row).

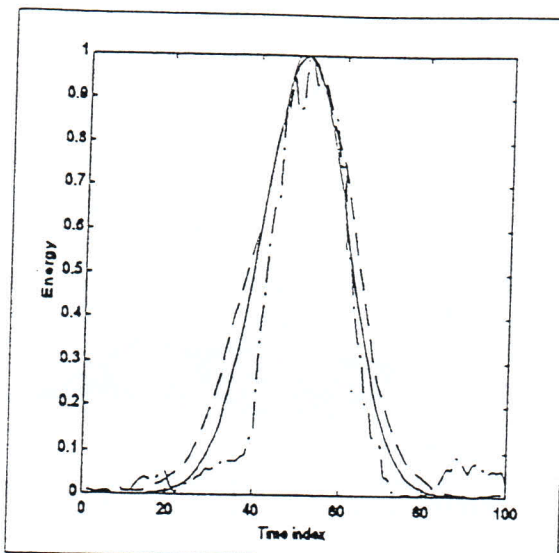


Figure 4. The 5th frequency slice of the theoretical Gabor logon (solid line), KS-TFD estimate (dashed line) and non-causal spectrogram (dash-dot line) for the 0db SNR case.

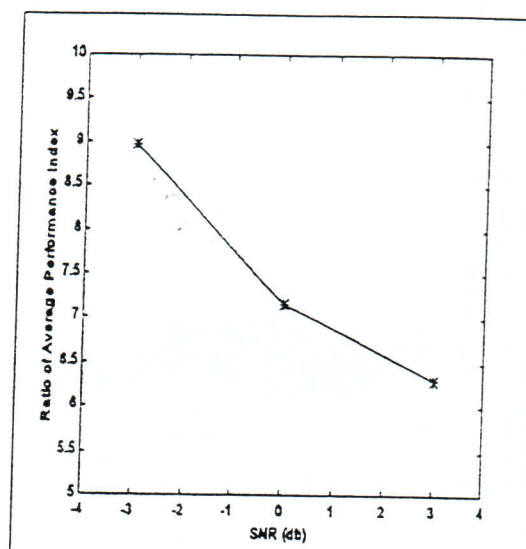


Figure 5. Comparison of performance of non-causal spectrogram to KS-TFD in the presence of noise; average of 30 independent realizations.